Journal of Volcanology and Geothermal Research 190 (2010) 11–24

Contents lists available at ScienceDirect

Journal of Volcanology and Geothermal Research

journal homepage: www.elsevier.com/locate/jvolgeores

The big crunch: Physical and chemical expressions of arc/continent collision in the Western Bismarck arc

Jon Woodhead [a,*], Janet Hergt [a], Mike Sandiford [a], Wally Johnson [b]

[a] School of Earth Sciences, The University of Melbourne, VIC 3010, Australia
[b] Pacific and Asian History Division, Australian National University, Canberra ACT 0200, Australia

ARTICLE INFO

Article history:
Received 8 July 2008
Accepted 1 March 2009
Available online 20 March 2009

Keywords:
geochemistry
geophysics
subduction
calc-alkaline
low-K tholeiite
arc–continent collision zone

ABSTRACT

The Western Bismarck arc of Papua New Guinea provides a unique setting in which to study both the seismic and chemical expressions of arc–continent collisional processes. Here collision has been oblique, occurring progressively along the arc from west to east, and currently centred around ~148°E. This progressive collision is reflected in sub-lithospheric seismic activity. Centroid Moment Tensor (CMT) focal mechanism data show that the north-dipping Solomon Sea slab subducting beneath New Britain can be traced westwards beneath the collision front. Beneath the Finisterre Ranges it defines an inverted "U"-shape with a steep northern limb extending to at least 250 km depth. Mechanical decoupling of the slab from the overlying lithosphere is indicted by a 90° rotation in *T*-axes at ~100 km. Further east, the seismic expression is less coherent suggesting progressive dismemberment and foundering of the slab, with maximum centroid depths shallowing to less than 125 km east of 144°E. When coupled with the known history of convergence, major, trace element and Sr-, Nd-, Pb-, and Hf-isotope compositions of volcanic rocks, provide further insights. The most dramatic geochemical expression of the collisional process is preserved in Pb-isotope ratios which peak in the zone of maximum convergence, reflecting the greatest slab-derived influence. Volcanic rocks in zones where convergence is complete show minimal expression of the slab-derived component although the fact that volcanism is still occurring suggests that either slab dewatering is not essential for initiating volcanism or that the process of dewatering continues long after subduction has ceased. Limited data from similar collision zones elsewhere suggest that these may be general observations applicable on a global scale and thus may provide a prediction of what might be expected in other areas of future convergence such as the Molucca Sea.

1. Introduction

The Bismarck volcanic arc is an intra-oceanic subduction system formed at the southern margin of the Bismarck Sea in the southwest Pacific Ocean. The arc can be divided into two sectors, east and west of longitude 148° E. The eastern part—the island of New Britain—continues to involve northward subduction of the small Solomon Sea plate, while the western arc now involves convergence between the Australian and South Bismarck plates in a zone of arc–continent collision. Magma genesis in the New Britain sector has been documented in some detail in previous publications (e.g. Johnson, 1977; Woodhead and Johnson, 1993; Woodhead et al., 1998, 2001); here we concentrate on the chemistry of magmas from the western collision zone, drawing upon previous work on New Britain for comparative purposes. The Western Bismarck arc constitutes a unique setting in which to study the process of arc–continent collision, since oblique convergence has shifted the collision front progressively eastward, allowing an unparalleled opportunity to study its temporal expression.

2. Geological setting and previous studies

Papua New Guinea is one of the most complex tectonic regions in the world characterised by multiple interactions along a variety of plate boundaries (e.g.,Tregoning et al., 2000; Wallace et al., 2004). The broad tectonic context is determined by oblique convergence between the Australian and Pacific plates, with complexity introduced by the partitioning of deformation among three smaller plates—the Woodlark, South Bismarck and Solomon Sea plates—and a host of diffusely deforming zones, located between these larger entities (Fig. 1). Interactions between the South Bismarck and Solomon Sea plates are particularly relevant to the current study.

The Solomon Sea plate is oceanic and is being subducted northwards beneath the South Bismarck plate at the New Britain trench (Fig. 1), producing subduction-related volcanism on New Britain (e.g. Johnson, 1979. Immediately to the west, convergence between the Australian and South Bismarck plates is accommodated by the Ramu–

* Corresponding author.
E-mail address: jdwood@unimelb.edu.au (J. Woodhead).

0377-0273/$ – see front matter © 2009 Elsevier B.V. All rights reserved.
doi:10.1016/j.jvolgeores.2009.03.003

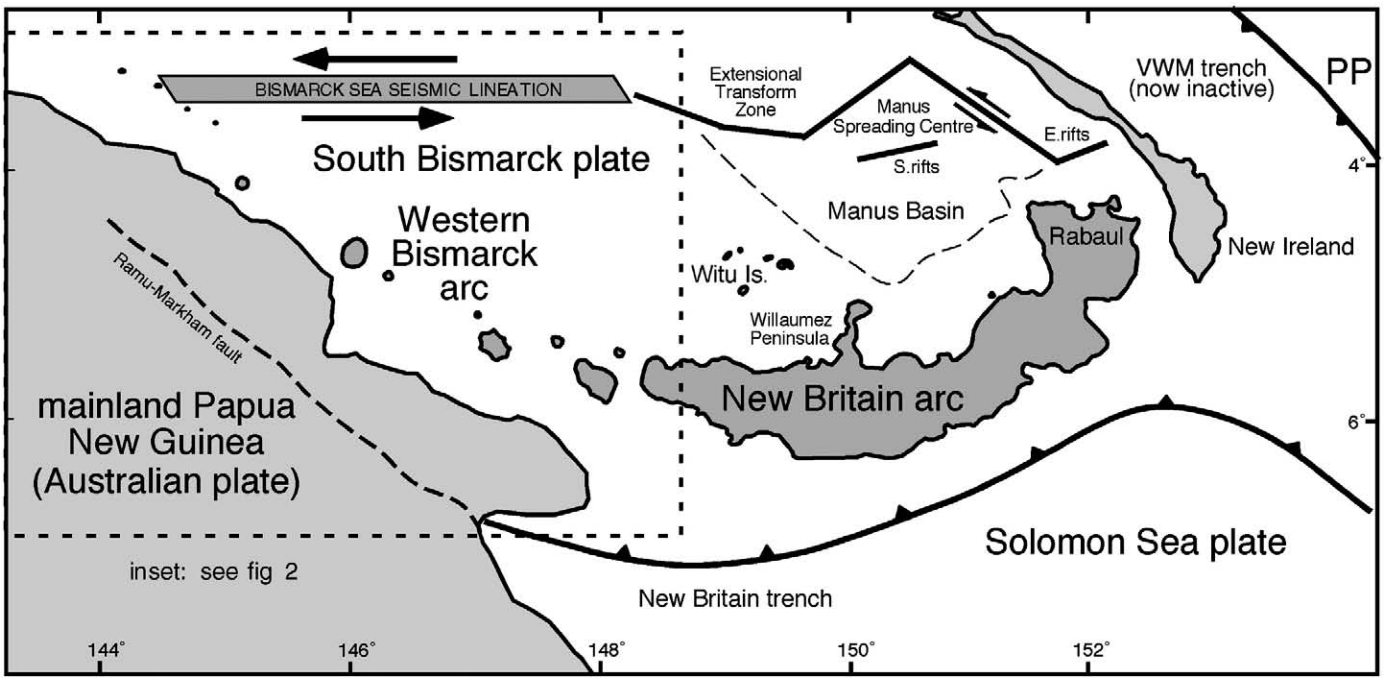

Fig. 1. Tectonic setting of the Bismarck Sea region. Currently, northward subduction of the Solomon Sea plate is occurring beneath the South Bismarck plate, with subduction-related volcanism on New Britain, and an area of complex back-arc spreading in the Manus Basin. The Western Bismarck arc extends to the west of New Britain and represents a zone of arc–continent collision where the Australian plate has collided with the trench in an oblique fashion. Convergence to the west of New Britain is accommodated along the Ramu–Markham fault zone. VWM = Vitiaz West-Melanesian, PP = Pacific Plate.

Markham fault zone (e.g., Pegler et al., 1995). Here subduction has also produced Quaternary volcanism: a chain of volcanic centres extends from the eastern end of New Britain westwards for nearly 600 km to the Schouten islands,[1] constituting the Western Bismarck arc (Fig. 2).

This outwardly simple picture is, however, complicated by the fact that arc–continent collision has occurred in the western segment, destroying the submarine trench, and leaving a remnant slab hanging approximately 100 km beneath the north-coast ranges of mainland Papua, continuous along strike with the New Britain seismic zone to the east (Abers and Roecker, 1991). No earthquakes with depths greater than 250 km have been reported west of New Britain (Cooper and Taylor, 1987), with no intermediate to deep events west of Karkar Island (Fig. 2). Remarkably, however, despite this, most of the volcanic centres within the arc, with the exception of Vokeo and Viai (Fig. 2), can be considered active or dormant. Of even greater interest is the observation that collision has been oblique, starting in the west and propagating southeastwards, producing progressive thrusting and uplift of the north-coast Adelbert and Finisterre Ranges (Johnson and Jaques, 1980). This uplift is continuing today on the Huon Peninsula which is notable for a magnificent flight of emergent Holocene coral terraces (Chappell, 1974). GPS observations suggesting that motion both across the Ramu–Markham fault (Wallace et al., 2004) and along the New Britain trench (Tregoning et al., 1998; Wallace et al., 2004) increases from west to east provide further support for this oblique convergence. A variety of methods have been used to deduce the apparent timing of the collision. Abbott et al. (1994) studied clastic sequences on the southern flanks of the Finisterre Range and concluded that the collision was initiated around 3–3.7 Ma, consistent with apatite fission track ages for unroofing in the eastern Papuan Fold belt of 4.0 ± 0.5 (Hill and Gleadow, 1989), whereas Gill et al. (1993) employed ^{10}Be studies to conclude that collision in the far west began in the early Pliocene and occurred within the last 1 million years in the region of 148° longitude, at the easternmost limit of the collision front (see below).

The Western Bismarck volcanic edifices are in all respects typical of subduction-related volcanoes but the Schouten islands in the far west are somewhat distinct in that they are volumetrically minor, form a volcanic line offset some 25 km from the remainder of the arc, and show morphological features suggesting that activity has migrated eastwards through the group (Johnson, 1977). The volcanoes of western New Britain and the islands and submerged reefs of the Bismarck arc appear to be arranged in a series of lines, which correspond to fault patterns on the Huon peninsula to the south (Johnson, 1977). This suggests at least a partial control by underlying fractures.

There has also been considerable debate, centred largely on the interpretation of geophysical data, as to whether the Solomon Sea plate is also subducting to the south as well as to the north, with the southwesterly dipping portion being termed the Maramuni arc (Dow, 1977). For example, Cooper and Taylor (1987) observed seismicity near the Finisterre Range which they note 'clearly defines the doubly subducted Solomon plate', whereas Abers and Roecker (1991) suggest that these seismic events 'do not require a southward subducting plate beneath the Papuan peninsula'. Pegler et al. (1995) showed that an intermediate-depth seismic zone 'forms an inverted U-shaped zone, with limbs dipping to the north and south', which they interpreted to represent seismicity along the double-subducting Solomon Sea plate, drawing an analogy with the Molucca Sea plate subduction system between Halmahera and northern Sulawesi (e.g., Widiyantoro and Van der Hilst, 1997). More recently Hall and Spakman (2002) failed to unambiguously resolve the proposed southward dipping slab in tomographic images, although their imaging does allow such a possibility. This debate continues.

The Manus Basin is a fast-opening marginal basin located north of the island of New Britain, with plate motion occurring along three

[1] The Schouten islands considered here are a group of small volcanic centres off the north coast of Papua New Guinea and should not be confused with the larger group of islands of the same name, located further to the west in the Irian Jaya Province of Indonesia.

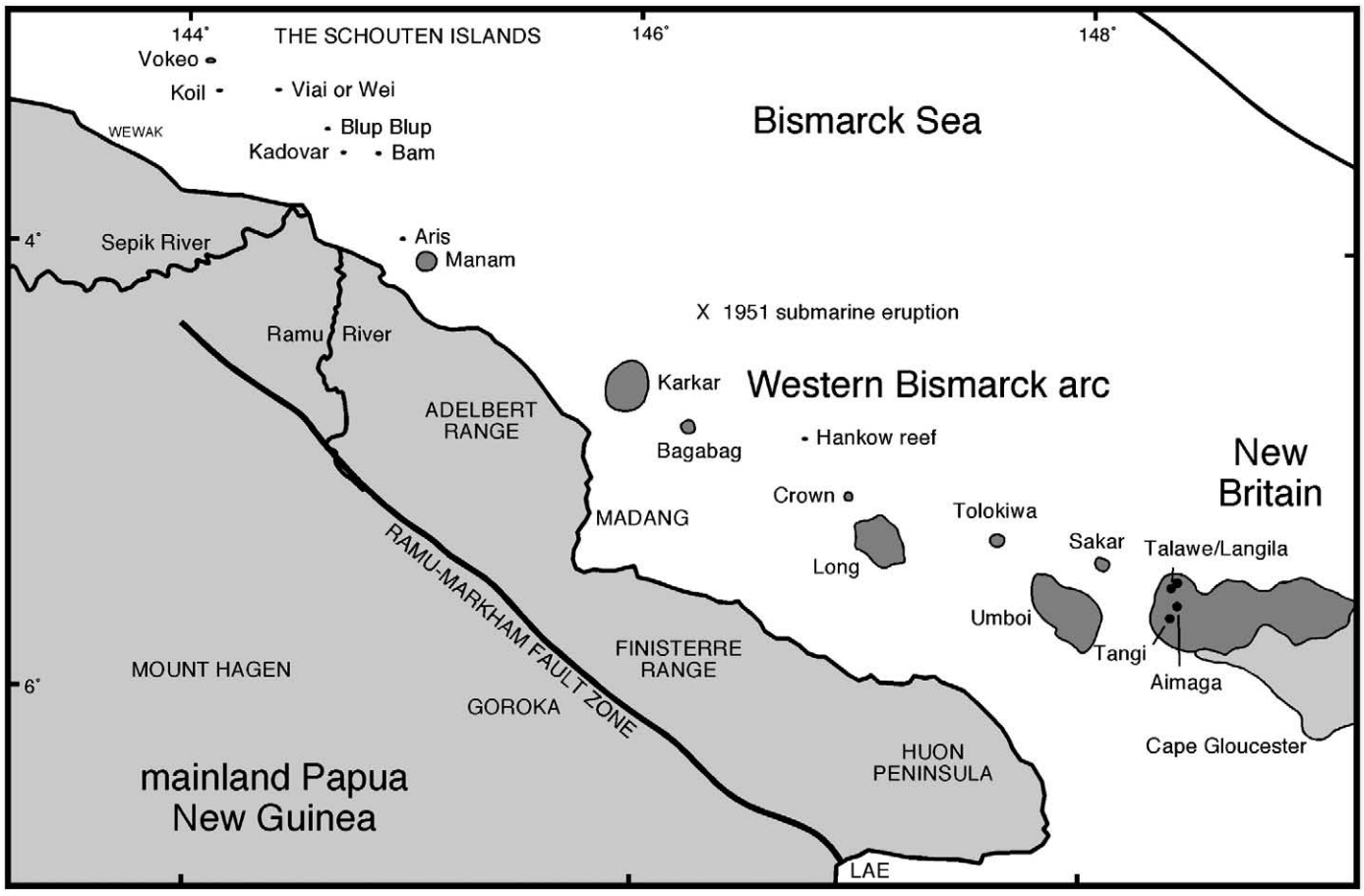

Fig. 2. Detail of the Western Bismarck arc region. In this study we consider the volcanoes on the west coast of New Britain to be part of the Western Bismarck arc. From here the subduction system extends westward to the Schouten islands.

major left-lateral transform faults and a number of extensional segments (Martinez and Taylor, 1996). Rather less is known about the nature of the Manus Basin spreading centre west of 148° longitude. A broad band of shallow seismicity approximately 20 km wide extends towards the north coast of mainland PNG (e.g. Denham, 1969), with focal mechanism solutions suggesting sinistral strike slip motions. This zone has been termed the Bismarck Sea Seismic lineation, and continues on land as a series of anastomosing faults which cut through the Toricelli and Bewani mountain ranges, and may accommodate some of the oblique convergence across the New Guinea trench (e.g., Johnson, 1979).

Johnson (1977) provided the first broad account of the chemistry of Bismarck arc lavas noting striking variations in alkali contents in passing along the arc, and the fact that the volume of eruptive products appears to decrease to the west. These features were attributed to changes in the rate of subduction along the arc with consequently differing thermal regimes from east to west in the subducting slab. Gill et al. (1993) provided ^{10}Be/B and U-series data for four locations in the arc as part of a wider study of recent Papuan lavas. Perhaps the most important aspect of the latter study was a novel use of ^{10}Be/^{9}Be data to provide age constraints on the progressive stages of arc–continent collision. These data indicate that the Adelbert Ranges became sutured to the Australian continent in the early Pliocene, the western Finisterre Ranges about 1.5 Ma ago and that collision in the east is less than a million years old. Furthermore Gill et al. (1993) observed that subduction-related element fluxes and apparent radium excesses reached maxima within the collision zone and that slab dehydration and permeable fluid flow continued for at least 3 Ma after collision commenced. These conclusions provide a well-constrained, temporally controlled tectonic framework for the interpretation of our new results.

3. Samples studied and analytical methods

Our sample suite consists of a subset of 27 samples representative of the 169 X-ray fluorescence analyses presented by Johnson and Chappell (1979) for the Bismarck arc, encompassing fifteen volcanic centres of the Western Bismarck arc between Cape Gloucester on New Britain island and the Schoutens. For these samples we present inductively coupled plasma mass spectrometry (ICPMS) trace element and Sr-, Nd-, Pb-, and Hf-isotope analyses (Table 1). XRF major element and selected trace element data are reproduced from Johnson and Chappell (1979) with the exception of two Manam Island samples which represent new analyses. In cases where applicable (e.g. Fig. 6) the full dataset of Johnson and Chappell (1979) has been employed.

Details of the XRF procedures used to acquire the major element data from Johnson and Chappell (1979) can be found in that reference; the two new analyses followed these same procedures (and were performed by Prof. Bruce Chappell, University of Wollongong). Trace elements were determined on a Fisons PlasmaQuad PQ2STE ICPMS at the Research School of Earth Sciences, Australian National University, using the method documented in Eggins et al. (1997). For the common USGS standards, reproducibility is generally better than 2% and analytical accuracy always within 5% for elements of mass $>^{77}$Se, Precision is better than 5% precision and accuracy within 10% for elements of lower mass. For the elements Rb, Sr, Y, Zr and Ba both XRF and ICPMS determined data are provided in Table 1. The agreement between these two methods is excellent.

Table 1
Major, trace element and isotope compositional data for the samples used in this study. Major elements and XRF trace elements reproduced from Johnson and Chappell (1979). All trace element values are in parts per million.

Sample	Volcano	SiO_2	Al_2O_3	Fe_2O_3	FeO	MnO	MgO	CaO	Na_2O	K_2O	P_2O_5	H_2O^+	Sc (XRF)	V (XRF)	Cr (XRF)	Ni (XRF)	Cu (XRF)	Zn (XRF)	Ga (XRF)	Rb	Rb (XRF)	Sr	Sr (XRF)	Y	Y (XRF)	Zr	Zr (XRF)	Nb
18NG-1043	VOKEO	57.60	16.00	2.75	6.15	0.17	3.85	8.54	2.20	0.48	0.10	1.21	33	272	8	7	79	82	14	6.7	6.4	381	389	15	13	32	34	1.66
18NG-1039C	VOKEO	61.50	16.20	1.98	3.05	0.09	4.60	7.60	2.75	0.73	0.16	0.65	19	139	70	36	43	44	13	7.8	10.4	575	615	10	10	66	71	4.32
18NG-973	BLUPBLUP	55.60	13.70	4.85	4.90	0.17	6.40	9.65	1.88	0.94	0.16	0.59	33	260	95	20	75	68	12	13.7	13.6	745	755	10	9	28	27	0.46
18NG-1031	VIAI	58.40	13.80	4.30	4.60	0.14	5.10	8.60	1.98	0.93	0.13	0.83	30	216	69	17	87	65	11.5	9.9	9.6	483	497	11	10	24	24	0.54
18NG-1034	VIAI	60.20	14.00	3.90	4.35	0.13	4.95	7.85	2.10	1.07	0.11	0.47	29	190	88	14	125	62	11	11.7	11.8	505	530	19	17	29	29	0.76
18NG-1010	BAM	54.90	16.50	4.80	4.25	0.16	5.41	9.40	2.25	1.36	0.19	0.36	31	269	35	14	40	63	13.5	18.9	18.6	694	720	12	11	31	30	0.5
18NG-1023	BAM	58.80	17.10	3.25	4.10	0.14	3.40	8.00	2.80	1.27	0.23	0.08	24	217	16	5	164	66	14.5	25.1	24.0	755	780	13	12	39	39	0.67
19NG-0953	BOISA	53.00	14.50	3.95	5.10	0.17	8.20	11.00	2.00	0.55	0.14	0.79	36	266	190	45	128	67	12.5	10.9	10.6	606	605	12	10	22	20	0.34
74710030	MANAM	53.50	16.60	4.40	3.95	0.16	6.40	9.70	2.75	1.03	0.20		32	320	129	48	149	78	14	16.3	15.5	549	570	16	15	42	43	0.75
MP87012M1	MANAM	52.04	16.07	9.58		0.17	7.29	11.32	2.53	0.65	0.09									8.8		538		13		23		0.38
MP92011M2*	MANAM	53.39	14.69	4.17	4.50	0.14	8.16	11.03	2.30	0.75	0.13									9.2		465	503	12	13	22	22	0.37
7471-0001	KARKAR	53.80	19.60	2.45	6.30	0.16	3.15	10.30	2.50	0.88	0.16	0.01	25	263	14	10	169	77	17	11.6	16.6	445	475	15	15	36	34	0.8
75710015	KARKAR	54.69	15.30	3.31	8.15	0.22	4.15	8.66	2.97	1.04	0.20		37	393	15	11	144	106	16.5	20.7	19.8	382	389	21	18	43	45	0.95
26NG-0788	BAGABAG	51.20	16.40	3.25	7.00	0.18	6.50	11.20	2.00	0.57	0.18	0.48	36	310	92	44	138	82	15	12.8	12.4	330	338	19	16	44	45	1.71
26NG-0787	BAGABAG	52.10	17.20	3.95	6.30	0.18	5.50	9.85	2.35	0.70	0.19	0.27	30	246	33	19	83	77	16	12.7	12.0	349	351	22	18	48	48	2.16
26NG-0763	CROWN	53.90	19.90	2.50	5.00	0.16	3.90	9.20	3.00	0.77	0.22	0.37	21	213	35	24	127	69	18	14.8	14.4	332	338	25	22	51	50	1.08
32NG-0754	LONG	48.10	17.90	4.75	6.65	0.20	6.85	11.50	1.99	0.72	0.15	0.40	36	338	33	28	161	77	16	6.0	7.4	758	775	13	12	23	24	0.44
32NG-0143A	LONG	51.40	17.40	2.75	8.05	0.22	4.40	10.90	2.35	1.33	0.25	0.17	29	318	8	7	144	99	16.5	23.8	22.5	690	690	19	16	45	45	0.89
32NG0124	LONG	56.70	15.10	2.80	8.20	0.25	3.10	6.95	3.25	2.25	0.39	0.07	28	255	5	4	243	133	17	38.0	36.5	629	640	29	25	76	74	1.47
32NG-0726	TOLOKIWA	48.90	16.70	3.95	6.65	0.19	7.50	11.90	2.15	0.88	0.22	0.16	36	273	143	61	101	69	15	9.9	9.2	556	570	21	18	35	35	0.68
32NG-0728	TOLOKIWA	50.70	17.70	4.05	5.70	0.18	6.00	10.90	2.50	1.16	0.33	0.17	29	279	72	29	97	73	16.5	18.1	17.0	584	585	26	22	55	54	1.09
32NG-0679	UMBOI	49.50	18.70	4.80	6.35	0.20	5.55	10.80	2.20	0.66	0.16	0.24	38	353	24	19	166	83	16	7.7	7.2	603	620	15	13	25	23	0.45
32NG-0111	UMBOI	49.90	12.00	3.65	6.05	0.18	14.90	10.50	1.62	0.56	0.11	0.25	39	259	1120	388	82	73	11.5	10.1	9.8	350	362	11	10	24	24	0.38
32NG-0682	UMBOI	50.00	15.80	4.75	7.25	0.21	7.05	11.00	1.84	0.53	0.14	0.30	46	334	53	26	121	79	14.5	6.8	6.4	460	487	14	12	20	20	0.33
32NG-0002C	TALAWE	50.50	17.00	4.50	6.50	0.20	5.60	9.80	2.50	1.00	0.18	0.88	34	317	24	20	225	93	17	11.4	10.8	670	650	18	15	38	39	0.63
32NG-0026D	AIMAGA	47.90	13.20	4.15	6.50	0.19	10.90	13.30	1.68	0.41	0.14	0.69	38	293	402	113	76	73	12.5	4.2	4.2	464	483	15	12	24	23	0.38
32NG-0031A	TANGI	49.70	13.80	4.20	6.80	0.20	9.35	12.00	1.90	0.84	0.17	0.32	41	322	257	85	142	78	12.5	9.9	9.8	518	530	14	12	28	27	0.51

Sample	Cs	Ba	Ba (XRF)	La	Ce	Pr	Nd	Sm	Eu	Tb	Gd	Dy	Ho	Er	Yb	Lu	Hf	Ta	Pb	Th	U	$^{87}Sr/^{86}Sr$	$^{143}Nd/^{144}Nd$	$^{206}Pb/^{204}Pb$	$^{207}Pb/^{204}Pb$	$^{208}Pb/^{204}Pb$	$^{176}Hf/^{177}Hf$
18NG-1043	0.26	92	85	3.86	8.75	1.30	6.01	1.65	0.57	0.36	1.91	2.25	0.52	1.56	1.57	0.25	0.90	0.11	1.97	0.42	0.22	0.703150	0.513060	18.686	15.530	38.289	0.283245
18NG-1039C	0.25	141	135	12.36	25.80	3.39	13.57	2.54	0.74	0.32	2.12	1.66	0.35	0.99	0.98	0.16	1.72	0.27	2.50	1.26	0.61	0.703202	0.513048	18.742	15.530	38.315	0.283160
18NG-973	0.43	150	155	7.35	15.40	2.14	9.20	1.92	0.58	0.26	1.68	1.52	0.34	1.03	1.05	0.17	0.81	0.03	5.10	1.03	0.57	0.703348	0.513047	18.650	15.537	38.291	
18NG-1031	0.45	137	135	4.34	9.14	1.33	5.78	1.41	0.43	0.26	1.41	1.62	0.38	1.14	1.19	0.19	0.69	0.04	3.78	0.56	0.38	0.703274	0.513028	18.681	15.536	38.305	
18NG-1034	0.56	165	165	6.91	12.19	1.91	8.46	1.99	0.63	0.41	2.33	2.55	0.60	1.83	1.84	0.30	0.88	0.05	4.08	0.76	0.48	0.703319	0.513056	18.671	15.526	38.269	
18NG-1010	0.68	144	145	6.49	14.00	2.04	8.99	2.00	0.62	0.31	1.87	1.81	0.41	1.24	1.25	0.20	0.88	0.04	4.29	0.81	0.51	0.703224	0.513045	18.695	15.559	38.387	0.283181
18NG-1023	0.92	186	170	8.07	17.40	2.48	10.64	2.29	0.68	0.34	2.11	2.00	0.45	1.36	1.40	0.22	1.13	0.04	5.92	0.98	0.66	0.703249	0.513070	18.671	15.540	38.342	0.283168
19NG-0953	0.66	150	160	5.18	11.30	1.66	7.40	1.76	0.56	0.29	1.73	1.81	0.41	1.23	1.26	0.19	0.66	0.02	4.00	0.60	0.33	0.703345	0.513005	18.689	15.564	38.438	
74710030	1.1	222	220	6.70	14.51	2.11	9.11	2.18	0.68	0.39	2.20	2.38	0.55	1.67	1.72	0.28	1.17	0.05	10.20	0.96	0.51	0.703205	0.513049	18.689	15.568	38.456	
MP87012M1	0.62	146		3.79	8.49	1.24	5.78	1.48	0.49	0.29	1.63	1.86	0.44	1.34	1.37	0.22	0.68	0.02	4.00	0.51	0.29	0.703265	0.513048	18.695	15.567	38.450	
MP92011M2*	0.67	151	181	3.75	8.62	1.23	5.56	1.43	0.47	0.27	1.52	1.71	0.38	1.17	1.21	0.19	0.66	0.02	3.93	0.52	0.28	0.703256	0.513055	18.683	15.558	38.434	
7471-0001	1.27	361		4.78	11.80	1.56	7.22	1.99	0.63	0.38	2.11	2.38	0.54	1.64	1.75	0.27	1.08	0.05	8.50	1.10	0.50	0.703924	0.513019	18.643	15.574	38.521	0.283159
75710015	2.1	420	415	6.74	14.80	2.11	9.60	2.49	0.80	0.49	2.79	3.07	0.71	2.15	2.19	0.34	1.30	0.06	10.50	1.46	0.64	0.703880	0.513020	18.667	15.590	38.564	0.283157
26NG-0788	0.45	106	100	7.19	15.20	2.28	10.06	2.53	0.78	0.46	2.64	2.87	0.65	1.91	1.86	0.29	1.23	0.11	3.10	0.96	0.39	0.703466	0.513016	18.762	15.557	38.489	0.283147
26NG-0787	0.25	90	85	6.32	14.51	2.17	10.09	2.61	0.86	0.52	2.90	3.24	0.74	2.22	2.20	0.35	1.39	0.14	2.21	0.86	0.37	0.703245	0.512985	18.787	15.573	38.540	0.283157
26NG-0763	0.2	134	130	7.13	15.45	2.21	10.10	2.64	0.90	0.57	3.04	3.60	0.83	2.55	2.57	0.41	1.42	0.07	4.23	1.06	0.47	0.703368	0.512981	18.741	15.571	38.531	
32NG-0754	0.28	90	85	4.50	10.77	1.68	8.15	2.16	0.79	0.36	2.20	2.13	0.45	1.32	1.25	0.19	0.72	0.03	3.53	0.46	0.25	0.703318	0.513026	18.707	15.568	38.472	0.283156
32NG-0143A	1.1	197	180	8.71	19.60	2.85	12.90	3.17	1.00	0.51	3.16	2.95	0.64	1.85	1.79	0.27	1.26	0.05	6.40	1.27	0.62	0.703324	0.513029	18.700	15.572	38.490	0.283136
32NG0124	1.78	306	285	13.50	30.00	4.42	19.60	4.91	1.43	0.78	4.76	4.52	0.99	2.86	2.79	0.44	2.08	0.08	10.00	2.05	0.98	0.703311	0.513032	18.692	15.564	38.469	
32NG-0726	0.11	80	85	6.08	14.70	2.26	10.60	2.78	0.93	0.54	3.14	3.29	0.73	2.17	2.06	0.31	1.09	0.04	1.84	0.51	0.27	0.703134	0.513027	18.700	15.544	38.350	
32NG-0728	0.36	109	100	9.87	22.50	3.32	14.80	3.66	1.14	0.66	3.76	3.96	0.89	2.63	2.53	0.40	1.53	0.07	2.65	1.06	0.53	0.703130	0.513028	18.708	15.550	38.387	
32NG-0679	0.32	93	85	4.86	11.10	1.67	7.90	2.13	0.74	0.38	2.31	2.34	0.52	1.55	1.51	0.23	0.75	0.03	3.27	0.48	0.22	0.703380	0.513031	18.709	15.557	38.425	
32NG-0111	0.45	91	85	4.46	9.78	1.48	6.73	1.74	0.54	0.30	1.75	1.82	0.41	1.22	1.16	0.18	0.70	0.03	3.60	0.73	0.34	0.703490	0.513013	18.670	15.560	38.450	0.283153
32NG-0682	0.27	71	70	3.70	8.61	1.40	6.69	1.95	0.66	0.37	2.17	2.23	0.49	1.42	1.36	0.21	0.64	0.02	3.04	0.35	0.19	0.703490	0.513014	18.706	15.561	38.443	0.283172
32NG-0002C	0.35	147	140	6.33	14.45	2.14	9.76	2.59	0.83	0.45	2.67	2.75	0.61	1.78	1.77	0.27	1.11	0.04	6.95	0.71	0.38	0.703426	0.513057	18.699	15.550	38.392	
32NG-0026D	0.05	53	55	3.24	7.89	1.27	6.18	1.83	0.67	0.37	2.12	2.32	0.52	1.50	1.38	0.21	0.69	0.03	1.64	0.23	0.12	0.703127	0.513050	18.672	15.529	38.296	0.283164
32NG-0031A	0.32	91	95	4.78	10.81	1.65	7.57	1.97	0.65	0.35	2.08	2.14	0.48	1.42	1.39	0.21	0.80	0.03	3.04	0.51	0.25	0.703133	0.513039	18.697	15.544	38.362	0.283179

For isotope analyses, hand-picked rock chips were first acid washed in hot 6 N HCl for around 30 min, rinsed in milli-Q water and finally dissolved in an HF/HNO_3 mixture in teflon beakers. Sr, Nd, and Pb were separated by conventional ion-exchange techniques, procedural blanks being negligible in all cases (total Pb blank was always less than 50 pg). Samples were run on a Finnigan MAT261 mass spectrometer at the Australian National University operating in static multi-collector mode. $^{87}Sr/^{86}Sr$ and $^{143}Nd/^{144}Nd$ were normalised to $^{86}Sr/^{88}Sr = 0.1194$ and $^{146}Nd/^{144}Nd = 0.7219$ respectively. Repeated analysis of the NBS 987 Sr and nNd-1 'in-house' Nd reference materials provided mean values of $^{87}Sr/^{86}Sr = 0.710198 \pm 4$ (2 s.e. for $n = 96$) and $^{143}Nd/^{144}Nd = 0.512200 \pm 3$ (2 s.e. for $n = 60$), the latter corresponding to a $^{143}Nd/^{144}Nd$ value for La Jolla Nd of 0.511899. Hf was separated by a two-stage ion-exchange procedure, and run on a Nu Plasma MC-ICPMS at the University of Melbourne as detailed in Woodhead et al. (2001). Results are provided relative to a $^{176}Hf/^{177}Hf$ value of 0.282160 for the JMC 475 reference material. Within-run precision (two standard errors of the mean) averages ±0.000008 for Nd-, ±0.000012 for Sr-, and ±0.000008 for Hf-isotope ratios respectively: errors for all samples fall within ±50% of these values. Measured Pb-isotope ratios were corrected for mass fractionation using a ^{207}Pb–^{204}Pb double spike, itself calibrated against the NIST SRM 981, and using the Richards (1986) preferred value of $^{208}Pb/^{204}Pb$ (36.700) for the former. For further details and a long-term assessment of this method, readers are referred to Woodhead et al. (1995), and Powell et al. (1998).

4. Discussion

4.1. Geophysical responses to arc–continent collision

Since the benchmark study of Pegler et al. (1995), the number of focal mechanism solutions in the Harvard Central Moment Tensor (CMT) database has almost doubled making it timely to reassess the seismic structure of this region. Here we briefly review the sub-lithospheric structure of the Western Bismarck collision zone as revealed by focal mechanisms, showing that these newly available data lend strong support for the main conclusions of Pegler et al. (1995), who postulated the existence of a seismogenic slab decoupled from, and foundering beneath the collision zone, with a north-dipping segment that is more than likely connected to a south-dipping segment.

The important first-order observation is that the distribution of sub-aerial volcanic activity throughout northern Papua New Guinea (PNG) is closely associated with belts of intermediate-depth earthquake activity, providing a direct link between magmatism and active subduction (Fig. 3). As has long been known, this is most evident in New Britain but is also the case for the Western Bismarck arc. The relationship between magmatism and intermediate-depth earthquake activity is less clear for volcanoes in the Central Papuan highlands and in eastern Papua, although a small number of intermediate-depth events (Fig. 3) suggests the existence of a weakly seismogenic slab(s) extending southwards from the Solomon Sea and the eastern part of the collision zone. As originally revealed by Pegler et al. (1995) detailed sections though the Bismarck arc show a pattern of seismicity consistent with an inverted U-shaped slab beneath 100 km depth. The new CMT solutions provide further support for this pattern although the 'aseismic' gap between 7°15′S and 6°20′S remains and, in this segment, allows for some ambiguity with regard to the existence of the southern limb. The new CMT data do however clearly confirm the steep north-dipping slab extending beneath Long Island (Fig. 2), where seismicity is particularly intense at depths of 150–250 km. Seismic activity in this northern limb is confined to a relatively narrow steeply dipping zone ~30 km in width consistent with the width of seismicity in many other seismically active slabs at intermediate depths (eg., Northard et al., 1996; Sandiford, 2008).

The focal mechanisms associated with the earthquakes at depths greater than 100 km show a distinctive pattern consistent with a double dipping slab system everywhere subject to down-dip tension (Figs. 4 and 5). The shallow, N–S trending *T*-axes at the top of this putative slab segment are associated with strike slip mechanisms (Fig. 5a) and dramatically contrast with the near vertical *T*-axes in the

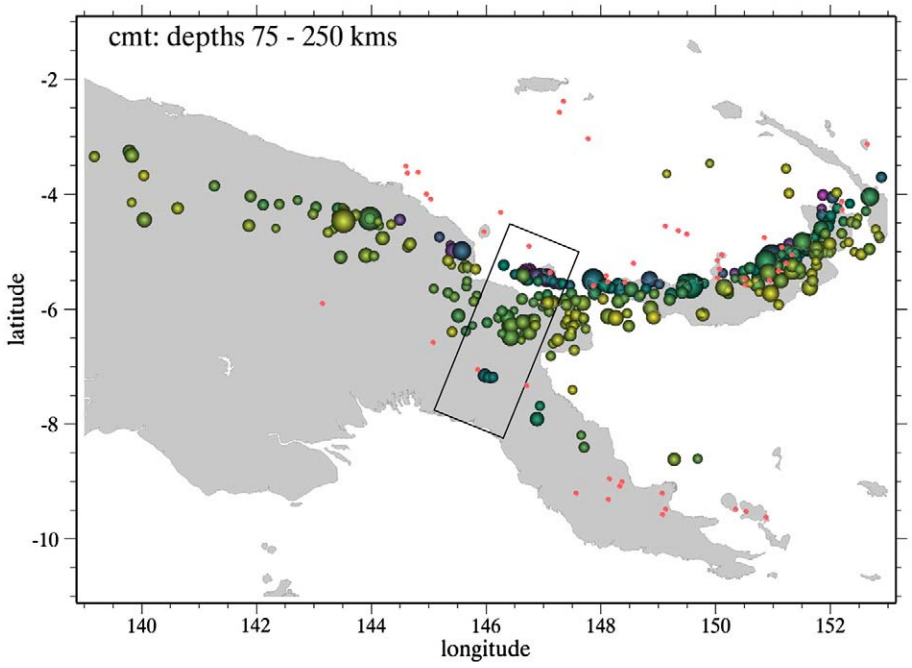

Fig. 3. Map of intermediate-depth CMT solutions inclusive to January 2008; data from the Harvard CMT catalog. Solutions are colour-coded for centroid depth from yellow (75 km) through green and blue to purple (250 km). Size is proportional to moment magnitude which ranges from Mw 5–7.6. Sub-aerial volcanoes are shown by red symbols. Note that the deepest centroid depths from 144°30′E to 147°E are consistent with a steep north-dipping slab system extending beneath the active segment of Western Bismarck arc. The location of the section illustrated in Fig. 5 is shown by the box.

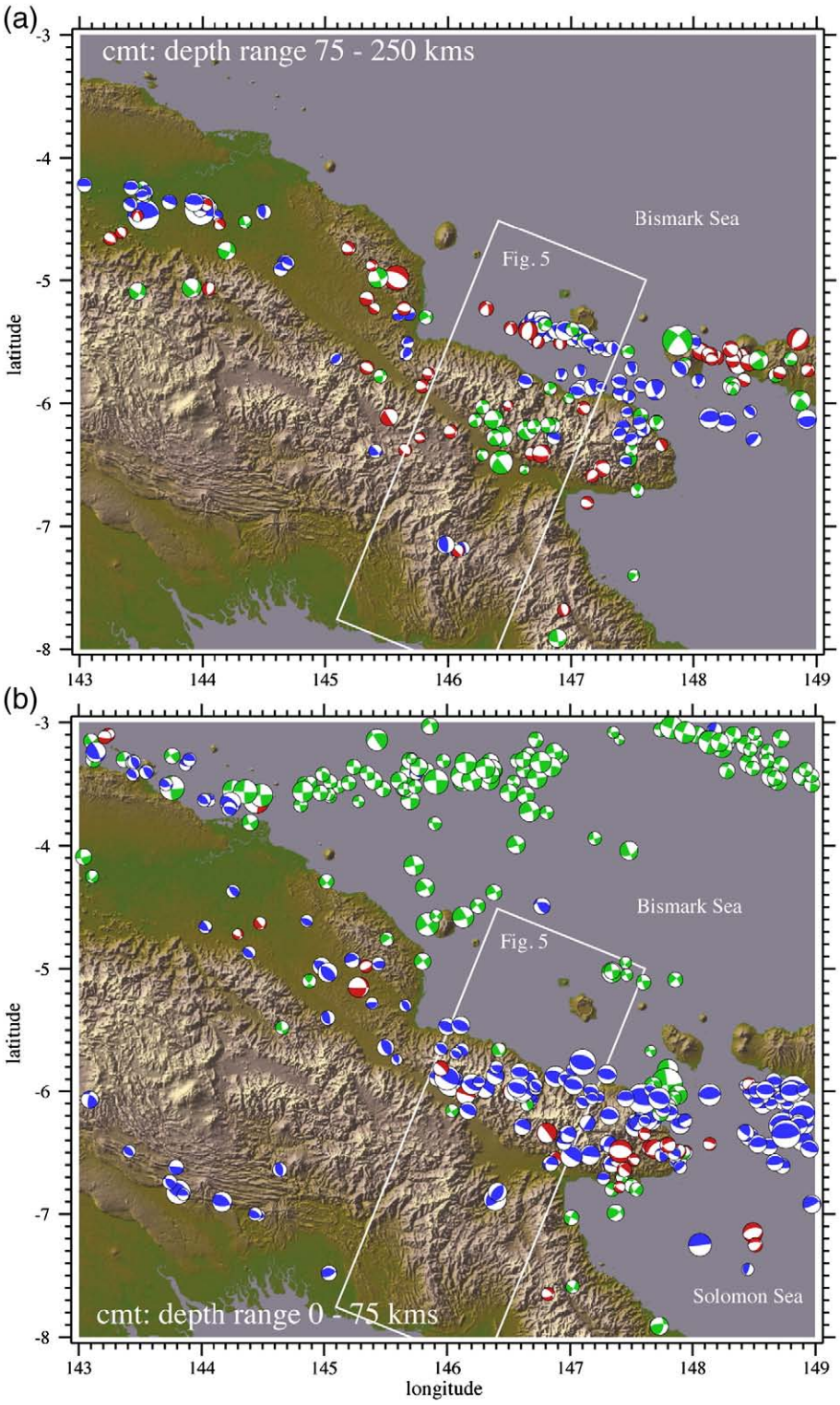

Fig. 4. CMT focal mechanism maps for (a) intermediate depths between 75 and 250 km and (b) shallow depths less than 75 km. The spheres have been colour-coded to represent normal (red), reverse (blue) and strike slip (green) solutions. The location of the section illustrated in Fig. 5 is shown by the box.

overlying lithosphere, associated with N–S lithospheric shortening in the collision zone (Fig. 4b). As noted by Pegler et al. (1995), this near 90° rotation of *T*-axes implies mechanical decoupling of the deeper seismic zone from the shallower zone.

West of the section shown in Fig. 5, the seismic expression of the slab is less coherent suggesting progressive dismemberment and foundering, with maximum centroid depths shallowing to less than 125 km east of 144°E; nevertheless there is clear evidence for a steep north-dipping zone of seismicity extending westwards to at least 144°30′E (Fig. 3), coincident with the western limit of volcanism in the Bismarck arc. Beyond 144°E the centroid depths are confined to less than 125 km and there is no clear asymmetry in the intermediate-depth earthquakes.

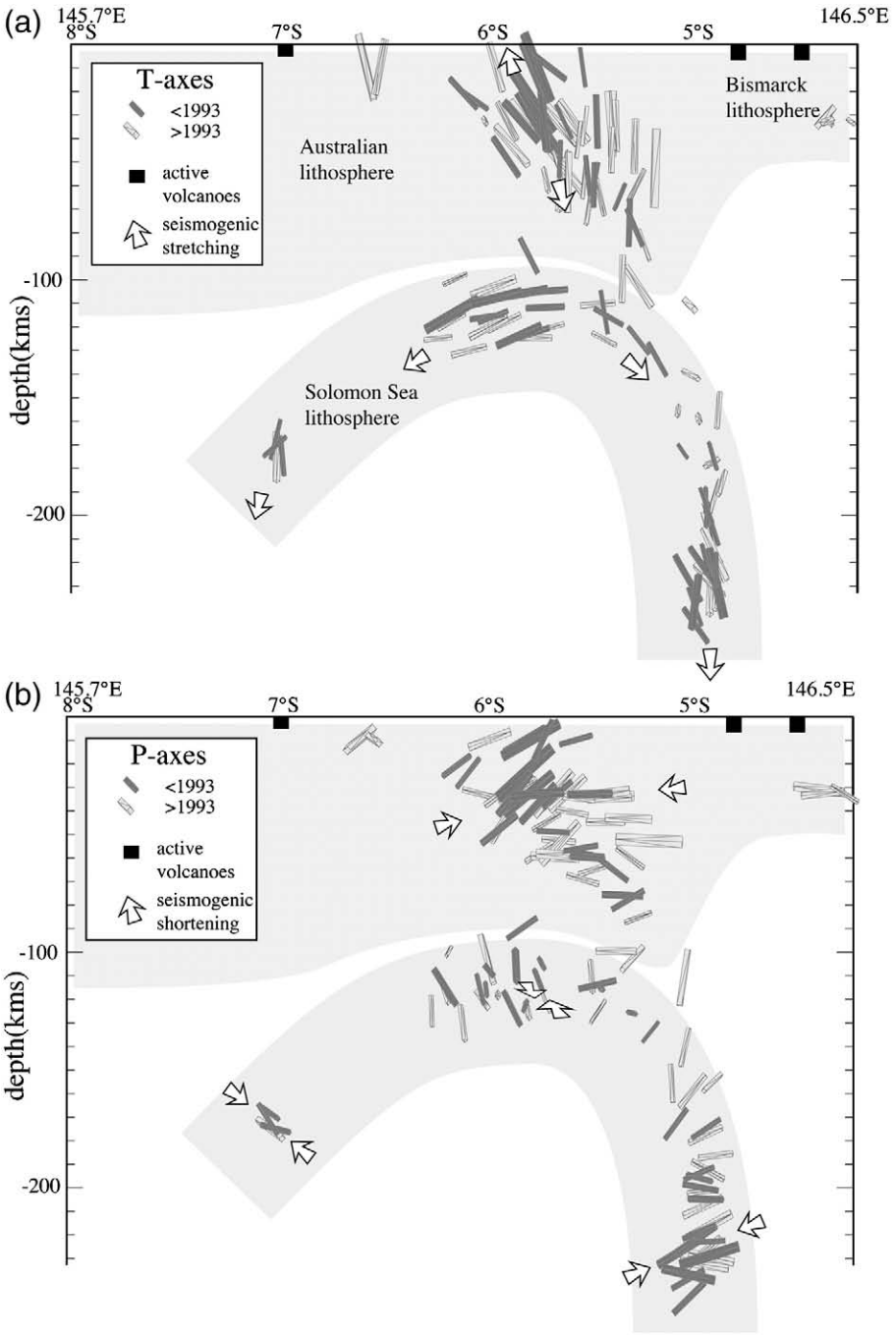

Fig. 5. a) *T*-axis and b) *P*-axis projections for CMT solutions shown in the boxed regions in Figs. 3 and 4. Solutions are marked according to age to discriminate the new solutions (light grey) that extend the older database (dark grey) used by Pegler et al. (1995).

4.2. Geochemical responses to arc–continent collision

4.2.1. A tale of two arcs

Although there remains some doubt as to whether the Tertiary arc terrane exposed on New Britain is analogous to the Tertiary arc sequences now being uplifted along the Finisterre and Adelbert Ranges of mainland Papua, the Quaternary volcanoes located along the north coast of New Britain can reasonably be considered a continuation of the Western Bismarck arc (Fig. 1) and can thus be used for comparative purposes. Such a comparison may provide some insight into the nature of the Western Bismarck arc prior to the onset of continental collision.

The classification of subduction zone volcanic rocks suites is, to quote Arculus (2003) 'plagued with inconsistency, with the terms having different meanings for different users'. In addition very few of the boundaries on commonly used discrimination plots have any clear petrogenetic significance and are often simply arbitrary constructs. Consequently we prefer not to assign the volcanic products of the New Britain and Western Bismarck arcs to any particular 'pigeonholes'. We do note as a point of historical significance, however, that the lavas of the New Britain volcanic front form a predominantly low-K suite and were defined as typical members of the 'island arc tholeiite' suite by Jakes and Gill (1970): Fig. 6. A far more informative aspect of this diagram, however, is the fact that there are clear differences between the volcanic rocks of the New Britain arc front and those of the Western Bismarck arc which are predominantly of medium-K character. Interestingly the volcanoes of Cape Gloucester (Langila,

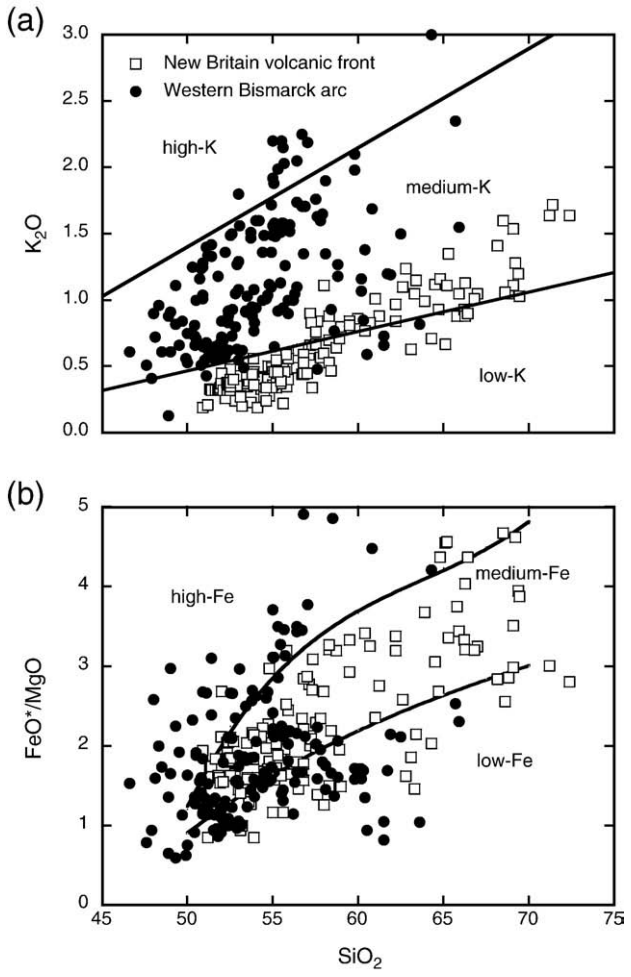

Fig. 6. K_2O–SiO_2(a) and FeO*/MgO–SiO_2 (b) for lavas of the New Britain and Western Bismarck arcs. Solid lines in (a) and (b) represent the compositional boundaries suggested by Gill (1981) and Arculus (2003), respectively.

Aimaga, Tangi, and Gloucester) appear consanguineous with the western arc, consistent with the notion that they share a similar genetic pathway. Consequently the volcanoes of Cape Gloucester, although geographically part of mainland New Britain, are considered herein products of the Western Bismarck subduction system and included in the present dataset.

The other widely used discriminant, which indicates the level of Fe-enrichment at any given degree of magmatic evolution, is shown in Fig. 6b. This diagram is also certainly useful in so much as it reflects the influence of H_2O content and oxidation state but it has also become embroiled in the confusion over the significance of the terms 'calc-alkaline' and 'tholeiitic', a nomenclature that has sparked many great debates in arc petrology. While the distinctions between New Britain and Western Bismarck arc volcanics in Fig. 6a would equate in the eyes of some workers to a tholeiitic–calc-alkaline transition, there is no clear distinction in terms of Fe-enrichment behaviour during magmatic evolution evident in Fig. 6b, resulting in an obvious conflict. In combination these two diagrams echo the conclusions of Arculus (2003) concerning potential misuse of the term 'calc-alkaline'. Such classifications were originally defined in order to describe volcanic rocks based upon limited datasets (particularly major elements) and we would suggest that, with the vast array of compositional information now at our disposal, they are of limited use and should largely be avoided. Issues of semantics aside, it is nevertheless important to account for the dramatic changes in composition in passing from New Britain into the Western Bismarck arc which may provide some insight into the phenomenon of arc–continent collision. Are these fundamental differences in chemistry a response to the nature and composition of the mantle wedge or subducting plate, or the processes of mass transfer between the two, or indeed a consequence of collisional processes?

The first question to address concerns the fertility of the mantle wedge, an issue made more intriguing by the fact that arc lavas from the New Britain volcanic front appear to derive from a mantle source which is highly depleted in many incompatible trace elements (Woodhead et al., 1998). The high field strength elements (HFSE) can be used to investigate these issues since it is widely held that they are less easily transported from the subducting slab, and thus provide a chemical 'window' into the mantle source region. Fig. 7a shows the comparison of Nb and Zr contents for Western Bismarck arc and New Britain volcanic front lavas, filtered to exclude samples with over 55 and 56 wt.% silica respectively (the filtering criterion was eased slightly for New Britain lavas to accommodate sufficient samples for display

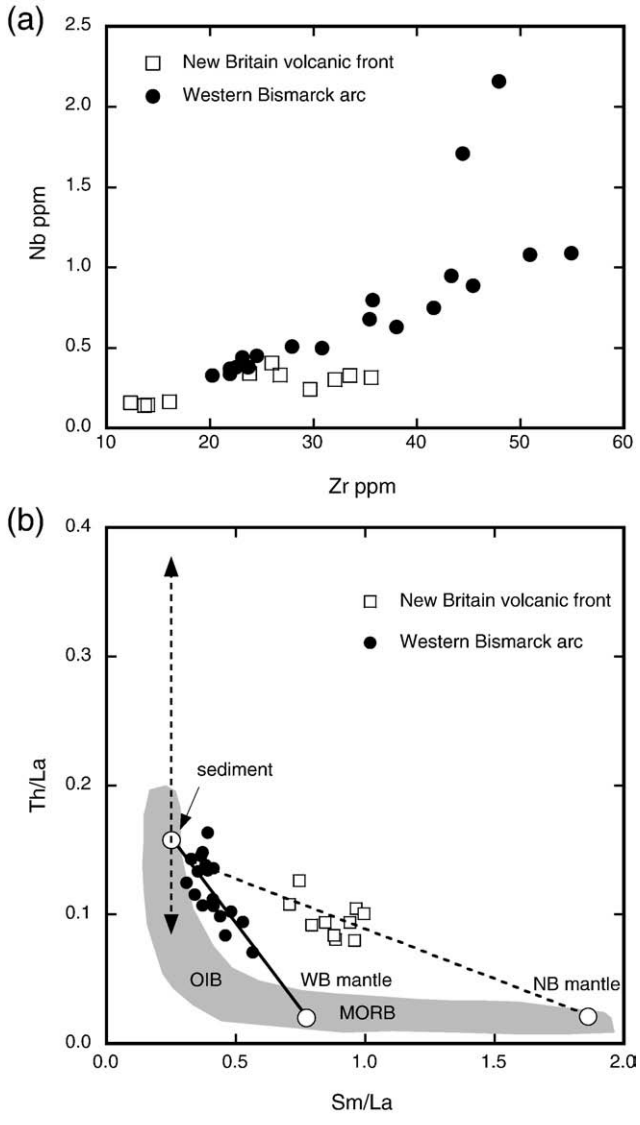

Fig. 7. (a) Zr ppm versus Nb ppm for least evolved samples from the Western Bismarck arc (<55 wt.% silica) and New Britain volcanic front (<56 wt.% silica). See text for discussion. (b) A Sm/La versus Th/La plot as used by Plank (2005) to distinguish mantle melting from sediment contamination effects. The broad shaded field represents the composition of MORB and OIB mantle sources while the vertical line shows the range of possible sediment compositions subducting beneath various arcs worldwide (both taken from Plank, 2005). The sediment composition chosen in our modeling (white circle indicated by arrow) is based upon an average sediment composition from the Solomon Sea plate (Woodhead et al., 1998). See text for discussion.

purposes but this does not change the structure of the data). The least evolved Western Bismarck arc lavas generally have higher contents of the HFSE than are seen in the New Britain volcanic front. In fact many of the Western Bismarck samples with lowest HFSE contents also derive from areas of this arc closest to the New Britain arc front. This suggests that the processes producing extreme elemental depletion in the New Britain volcanic front lavas, which Woodhead et al. (1993) ascribed to prior melt extraction in the back-arc, have not operated to the same extent on the mantle source of the Western Bismarck lavas, except at its most easterly end. This seems a perfectly reasonable observation given that the Manus Basin spreading centre does not extend westward beyond the island of New Britain (Fig. 1).

These conclusions are confirmed in a plot of Sm/La versus Th/La (Fig. 7b) as employed by Plank (2005). In such a plot arc magmas generally form linear arrays between mantle and sediment end members; at one end of these arrays the Sm/La ratio tells us something about the nature of depletion in the mantle wedge whereas, at the other, the Th/La ratio provides constraints on the nature of the subducting sediment component. In this figure MORB and OIB mantle sources are shown as a shaded field while the vertical line indicates the range of possible sediment Th/La ratios (all at low Sm/La). As shown in Fig. 7b the New Britain arc front and Western Bismarck arcs plot in quite different regions of this diagram. The New Britain data are rather diffuse and so it is difficult to produce a precise regression through the analyses (the putative line we have drawn is based upon an average sediment composition from the Solomon Sea of Woodhead et al., 1998). It is clear, however, that Sm/La ratios are significantly higher when compared to the Western Bismarck (and indeed most arc) lavas hinting at a very depleted mantle source, entirely in keeping with the observations made above. In contrast, for the Western Bismarck lavas Th/La and Sm/La ratios are well correlated allowing a more precise estimation of the composition of both mantle and crustal components. The Sm/La ratio of ~0.75 in the mantle end member suggests a relatively fertile mantle source similar to that found beneath the Aleutian, Vanuatu and Honshu arcs, for example (Plank, 2005), and lying somewhere between the composition of N-MORB (~1.0) and E-MORB (0.4).

Unfortunately, we do not have any direct samples of the sedimentary materials subducted beneath the Western Bismarck arc during the collision but Fig. 7 does provide some insight into their likely composition. The extrapolated Th/La ratio of ~0.175 is somewhat lower than that of bulk continental crust (0.27 ± 0.05) and the 'average arc' (0.25 ± 0.07) of Plank (2005), suggesting possible dilution with volcanogenic material. We might expect that the Australian plate, prior to collision with the South Bismarck plate, carried such a signature, due to the sediment load shed from mainland Papua New Guinea by its northward directed river systems which, at the present day, is largely composed of arc-derived debris. In further support for such an inference this low Th/La sediment end member seen in the Western arc lavas appears very similar to average sediments from the Solomon Sea (Woodhead et al., 1998) which also contain a substantial PNG-derived volcaniclastic input (Crook, 1987).

Fig. 8 shows the Pb-isotopic compositions of the Western Bismarck lavas in a regional context. These samples contain relatively radiogenic Pb (displaced to higher $^{206}Pb/^{204}Pb$ and $^{207}Pb/^{204}Pb$ compared with Manus Basin MORB) with a strong 'crustal' signature evident, similar to Pb compositions found in the Solomon Sea sediments noted above. This is in marked contrast to the lavas from New Britain which define a shallower array extending into the MORB field. The New Britain Pb-isotope data have been interpreted as a mixture of mantle Pb and Pb derived from fluids expelled from subducting oceanic crust (e.g., Woodhead et al., 1998). The Western Bismarck lavas, in contrast, seem to contain Pb with a greater sediment influence.

In summary, therefore, we note that the Western Bismarck and New Britain arcs, although contiguous along strike and most likely formed simultaneously, exhibit very different geochemical character.

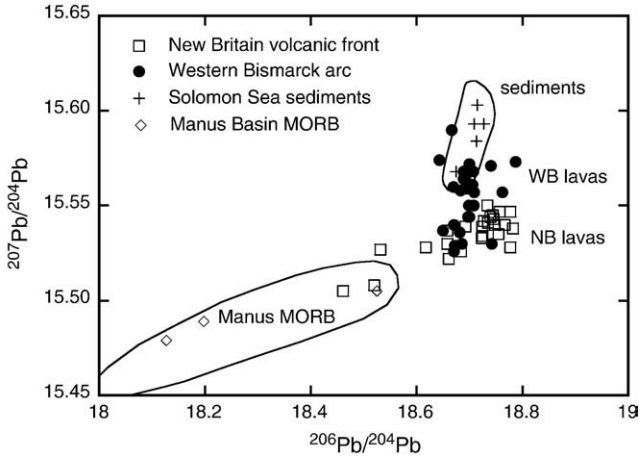

Fig. 8. Pb-isotope compositions of the Western Bismarck—WB (filled circles), New Britain—NB (open squares) and Manus Basin MORB (open diamond) lavas, compared to sediments from the Solomon Sea plate. All data from this study and Woodhead et al. (1998). Western Bismarck lavas display enhanced 'sediment' signatures when compared to New Britain lavas, reflecting a much greater crustal input.

The New Britain mantle source is highly depleted, most likely because of prior melt extraction in the Manus Basin back-arc, and the lavas reflect a subduction-component probably dominated by slab-derived fluids, with minor sediment input. In contrast, lacking an associated back-arc, the Western Bismarck lavas are formed from a much more fertile mantle source upon which is superimposed a strong crustal-Pb signature, which is most likely to reflect the involvement of continent-derived detritus shed from the New Guinea mainland during collision.

4.2.2. Geochemical variation along the Western Bismarck arc

Having used the comparison with the relatively well-studied New Britain arc in order to establish baseline constraints on the nature of the components contributing to magmagenesis in the western arc, we can now investigate variation in geochemical responses passing west along the Western Bismarck arc itself, which may ultimately be related to the oblique collision process, and thus provide some insight into its progressive effects. Of the major elements, SiO_2 contents clearly increase to the west away from Cape Gloucester whereas TiO_2, FeO, MnO (the latter not shown), and CaO abundances fall, particularly west of Bam in the Schouten islands (Fig. 9). The other major elements do not show distinct trends.

These variations suggest a decrease in the degree of melting, or greater extent of fractional crystallisation in passing west, especially within the Schouten islands. However, with the exception of three samples in the east which appear to have accumulated plagioclase, there is no noticeable variation in europium anomaly (Eu/Eu*) along the arc (Fig. 9). This suggests little variation in the extent of plagioclase fractionation along the arc and, although we cannot rule out significant variations in olivine and pyroxene fractionation, is also consistent with a control by degree of partial melting. Furthermore the Sm/La ratio, which has already been presented as an index of degree of mantle melting decreases monotonically (Fig. 10) and, finally, as Johnson (1977) notes, the size of volcanic edifices and eruption rate decreases markedly towards the west. All of these factors lend weight to the hypothesis that the degree of mantle melting falls dramatically in passing east to west, most likely in response to collapse of the typical subduction regime during prolonged arc–continent collision.

In contrast typical indicators of subducted slab contributions to melting such as Sr/Nd, Ba/La, Th/La, and Pb/Nb ratios, show a rather different but nevertheless systematic behaviour (Fig. 10). These

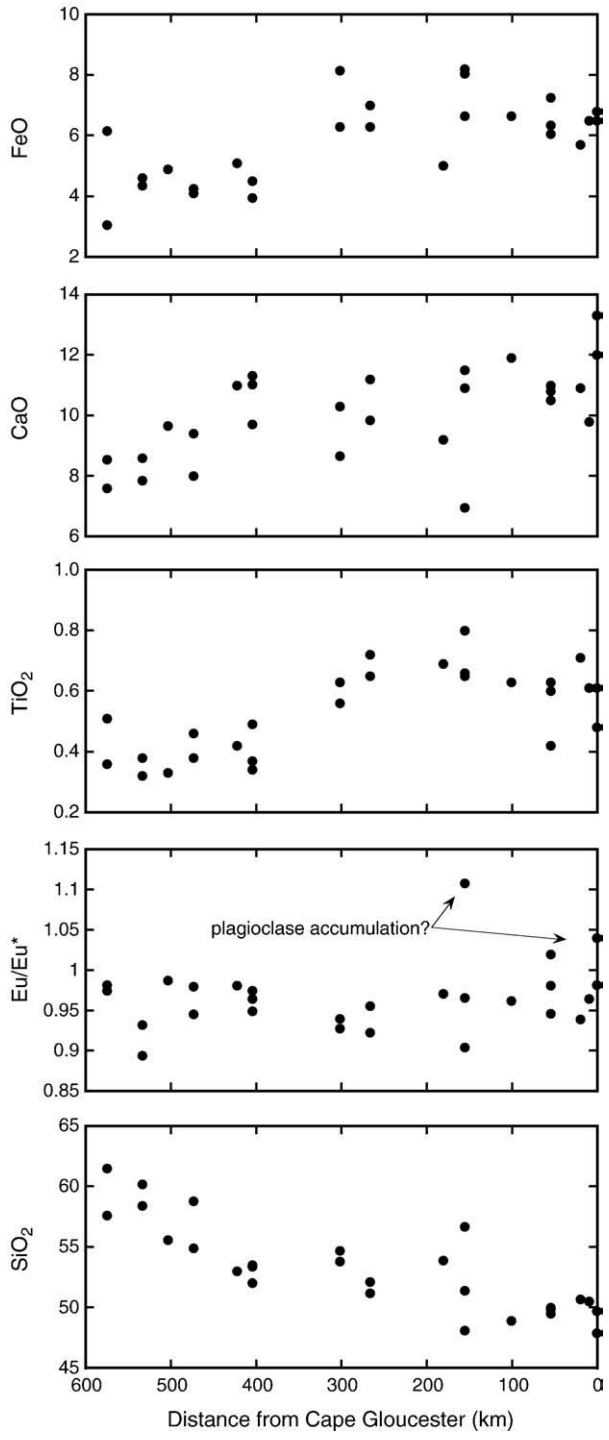

Fig. 9. Selected major and trace element parameters versus distance along the Western Bismarck arc. See text for discussion.

typically exhibit maximum values in the middle of the arc around 300–400 km from Cape Gloucester (corresponding to the islands of Manam and Karkar) and then steep declines in passing west to the Schouten group. To the east they typically fall but often to a more variable extent than in the west. Isotopic variations are shown in Fig. 11 and it is clear that, with the exception of Hf, which is relatively constant along the arc, these exhibit many similar characteristics. Most distinctive are the variations in $^{207}Pb/^{204}Pb$ and $^{208}Pb/^{204}Pb$ and to a lesser extent $^{143}Nd/^{144}Nd$ and $^{87}Sr/^{86}Sr$ which all show strong crustal signatures in the centre of the arc. Such highly radiogenic compositions can be interpreted as a response to arc–continent collision where increased proximity to a crustal source can dramatically increase the proportion of continent-derived detritus delivered to the subducting slab. The only remaining ambiguity is the question of why the apparent maxima in crustal, slab-derived signatures appear mid-way along the arc when collision is thought to be complete up to 148° longitude. We suggest that the present distribution of signatures is related to the relatively slow response of the subduction system to such effects. The distance from the trench, down-slab, to the zone of slab dehydration and melting is ~250 km, based upon the seismic imaging shown in Fig. 5. Although the convergence rate, pre-collision, is unknown, at the

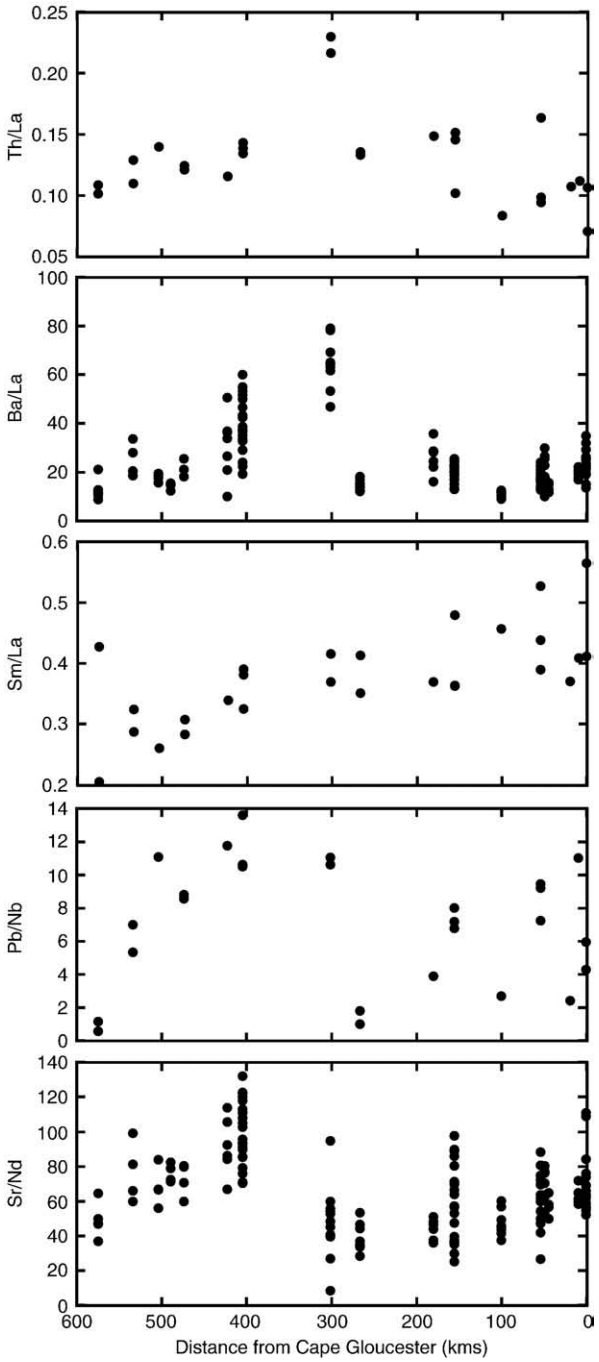

Fig. 10. Selected trace element ratios versus distance along the Western Bismarck arc. These plots are based predominantly upon ICPMS data but, in the case of the Sr/Nd and Ba/La plots, these have been supplemented by additional XRF data from Johnson and Chappell (1979). See text for discussion.

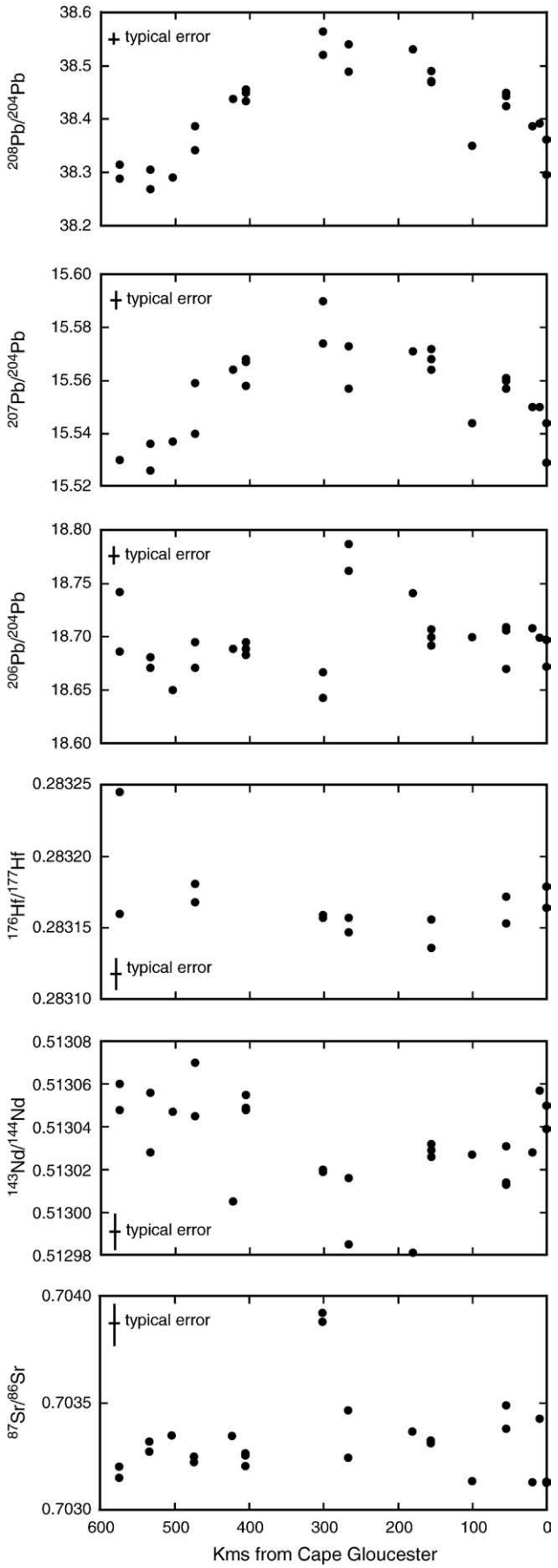

present time, convergence in the system varies from a few mm in the west to around 61 mm/yr in the east (Wallace et al., 2004). Thus, if we consider, for example, a possible pre-collision convergence rate of 10 mm/yr, it could take ~2.5 million years for any subducted crustal products to reach the zone of melting (thereafter slab dehydration and melt transport to the surface are relatively rapid processes e.g. Gill et al., 1993). It may be that we are only now seeing the effects of collision 2.5 million years ago in the volcanic products erupted at the surface. Those lavas erupted in the east of the arc have yet to bear witness to this event and are still recording 'normal' subduction signals from a pre-collision time. Only in the centre of the arc are we now seeing peak collisional signatures. The greatly diminished crustal signals observed in the Schouten islands could be a reflection of the fact that collision here occurred >3 million years ago (Gill et al., 1993) and thus we might expect that any slab-derived components have been melted out of the system. This concept is consistent with the diminutive size of the volcanic edifices in this part of the arc suggesting limited partial melting at the present time. Given the chemical and morphological differences observed between the Schouten islands and the rest of the arc, however, it is also prudent to consider to what extent magmatism on these islands is a consequence of proximity to the Bismarck Sea/Pacific plate boundary (see Fig. 1). Johnson (1977) considered that this boundary, which is marked by either a single or multiple anastomosing faults, may have been located to the west of Vokeo when sub-aerial magmatism first commenced, and that it has moved eastwards by activation of new faults, to its present position passing along the way through the most easterly of the Schoutens (Kadovar, Blup Blup and Bam). Thus at the present day the islands of Vokeo and Viai would no longer be associated with the Indo-Australian/Bismarck plate system, which could possibly explain why they have become volcanically inactive. While such a model accounts for the apparent migration of volcanism within the Schoutens, an implication is that the plate boundary has had little chemical effect on magmatism since the still active Schoutens have very similar chemistry to Vokeo and Viai, despite being originally some distance from the plate boundary.

4.3. Comparison with other collisional settings

Regions of arc–continent collision are rare but at least two other examples, the Sunda–Banda and North Luzon arcs, allow comparison with the Western Bismarck arc data. The Sunda–Banda system displays many similarities with the Bismarck arc with the Indian–Australian plate converging obliquely along the arc (northwest directed convergence) with a rate of around 7–8 cm/yr. While oceanic crust is being subducted in the west beneath the Sunda arc, Australian continental crust has entered the subduction zone in the eastern Sunda/Banda segments. The Indian–Australian plate is seismically defined to a depth of more than 600 km (McCaffrey, 1989) but shallow earthquake foci are absent near Timor, where the collision is believed to have begun due to an assumed 'bulge' in the pre-subduction Australian margin. There remains some debate as to when collision began with estimates varying from 3 Ma (e.g., Abbott and Chamalaun, 1981) to as long ago as 8 Ma ago (Berry and McDougall, 1986) but such figures are of the same magnitude as the inferred collisional history in the Western Bismarck arc. We might infer, however, from the lack of deep earthquakes throughout the Western Bismarck arc, that collision there is in a slightly more advanced stage.

Van Bergen et al. (1993) have presented a synthesis of isotopic results from a Sunda–Banda arc traverse (see also Elburg et al., 2005, Fig. 6 for a detailed compilation of Pb-isotope data from this transect). The isotopic variations observed in this setting have many parallels

Fig. 11. Sr-, Nd-, Hf-, and Pb-isotope ratios versus distance along the Western Bismarck arc. See text for discussion.

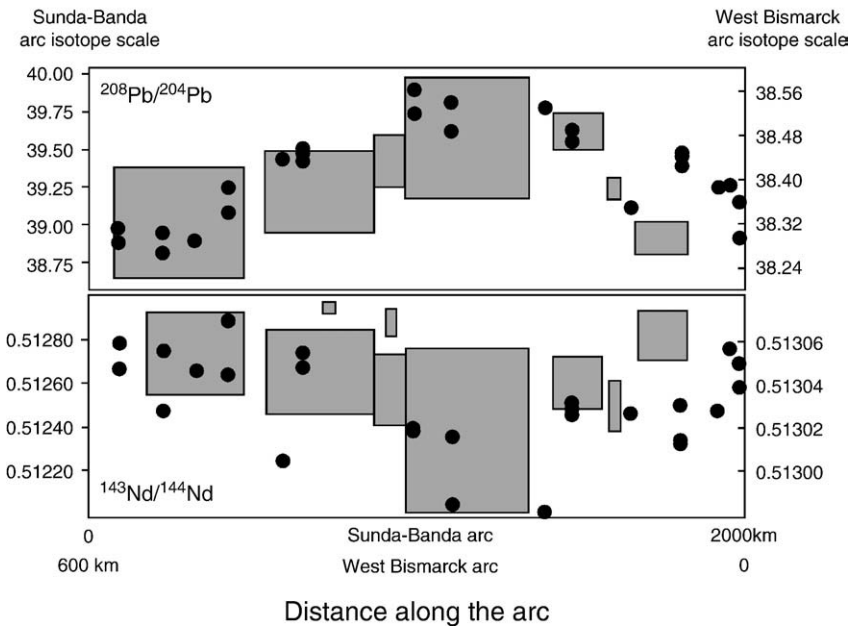

Fig. 12. Comparison between the Nd- and Pb-isotope data from this study and those presented by Van Bergen et al. (1993) for the Sunda–Banda arc collision zone of Indonesia. The transects along the two arcs are shown superimposed but, to achieve this, different scales have been used for both the horizontal and vertical axes each arc; *y*-axis scales for Sunda–Banda are shown on the left hand side, those for West Bismarck on the right hand side. For the horizontal scales, that for Sunda–Banda is shown heading east from Bali, for the Western Bismarck arc, variations are shown heading west from Cape Gloucester. Note the similarity in structure, albeit at a different scale, between the two collisional environments. See text for discussion and also Elburg et al. (2005) for a more detailed analysis of Pb-isotope variation along the Sunda–Banda collision zone.

with the Western Bismarck arc data. In particular Van Bergen et al. (1993) observe the most radiogenic, 'crustal' isotope ratios of Sr, Nd, and Pb in the sector north of Timor, with gradationally less radiogenic signatures to the east and west. They note that at least some of this isotopic variation may be a reflection of changing sediment compositions on the subducting plate with greater proportions of continent-derived detritus at the leading edge of the subducting continental margin. Fig. 12 illustrates the similarity, albeit at different scales, between the Sunda–Banda and the Western Bismarck Nd- and Pb-isotope variations. In the case of the Sunda–Banda arc, subducted terrigenous sedimentary material with distinctive Sr-, Nd-, and Pb-isotope signatures is likely to have been derived from the Proterozoic crust of northern Australia. In contrast material eroded from the Papuan mainland is likely to be derived from the Tertiary arc-related terrains exposed there. Consequently in the latter case the isotopic signature from the subducted sediment can be assumed to be far more primitive and less distinctive. For this reason the isotopic shifts seen in the Western Bismarck volcanics are far more subtle than those found in the Sunda–Banda arc (ranges in $^{208}Pb/^{204}Pb$ of 38.25 to 38.55 and 38.7 to 40.0 respectively). Indeed it is debatable whether the former would be noticeable without the high precision analytical procedure adopted in this study. Nd variations within the Western Bismarck arc are also minor relative to the Sunda arc ($^{143}Nd/^{144}Nd$ ranging from 0.51298 to 0.51307 and 0.51200 to 0.5129 respectively) but, once more this observation is readily explained by the nature of the subducting crustal material.

A further comparison is provided by the North Luzon arc. The tectonic setting here is complex but collision of the northern Luzon arc with Taiwan commenced in the late Miocene, was complete on Taiwan in the Pleistocene and continues today further south. Yang et al. (1994) present details of a combined isotope and trace element study of the Taiwan lavas and, once more a clear picture emerges of greatly enhanced subduction signatures within the collision zone, reflected in more radiogenic isotope ratios. These variations were interpreted as a response to a greater proportion of continent-derived detritus being subducted at the time of collision. Furthermore distinct temporal trends occur suggesting that lavas younger than 4 Ma are dramatically enriched, coinciding with the time of initial collision between the arc and continental margin. These conclusions are also consistent with the data presented in McDermott et al. (1993).

5. Conclusions

The great tectonic complexity of the Papua New Guinea region has resulted in a remarkable natural laboratory for the study of plate convergence and subduction. The Western Bismarck arc, situated off the north coast of Papua New Guinea preserves a valuable record of oblique and gradual arc–continent collision with the Australian plate spanning several million years.

Available seismic data reveal a steeply dipping and well-defined subducting slab in the east which appears decoupled from the overlying lithosphere. There is also convincing evidence for a southward dipping limb, which might explain some of the enigmatic volcanic activity in central Papua. Westwards the seismic expression of the north-dipping slab becomes increasingly diffuse suggesting that it is being gradually dismembered.

Chemically the Western Bismarck arc is distinct from contemporaneous volcanism on New Britain. We have argued that this is because the mantle sources beneath New Britain are more depleted than those from which the Western Bismarck volcanics have derived and that the latter have incorporated an increased sedimentary input from the subducting slab.

Systematic chemical variations occur along the Western Bismarck arc and these are thought to be a response to the oblique convergence. In particular we observe peak 'crustal' signatures in the middle of the arc and these are subdued among the Schouten islands in the far west. We suggest that, in the far west, all components derived from the subducting slab have been 'melted out' of the system. In the centre of the arc, the enhanced subduction signature, derived from increased sediment load shed from the converging Australian plate, has only recently reached the zone of melting. In the east, the geochemical response of the system is still in its pre-collisional state. Comparison with other collisional settings worldwide suggest that these features may well be common to all zones of arc–continent collision and thus

may provide a prediction of what might be expected in other areas of future convergence such as the Molucca Sea.

Acknowledgements

Samples were collected as part of a Geoscience Australia (formerly Bureau of Mineral Resources) mapping program in the 1970s. Bruce Chappell produced the XRF data for the original Papua New Guinea studies and Steve Eggins is thanked for his assistance with the ICPMS analyses at ANU. Detailed reviews from Richard Price and one anonymous reviewer helped to improve the manuscript significantly. Finally, it is a pleasure to acknowledge the many and varied contributions made by John Gamble over the years; his passion for subduction zone volcanism and animated discussion, particularly over a bottle (or two) of fine red wine, has been inspirational.

References

Abbott, M.J., Chamalaun, F.H., 1981. Geochronology of some Banda arc volcanics. In: Barber, A.J., Wiryosujono, S. (Eds.), Geology and Tectonics of Eastern Indonesia. Indon. Geol. Res. Dev. Centre Spec. Publ., vol. 2, pp. 253–268.

Abbott, L.D., Silver, E.A., Thompson, P.R., Filewicz, M.V., Schneider, C., Abdoerrias, C., 1994. Stratigraphic constraints on the development and timing of arc–continent collision in northern Papua New Guinea. J. Sediment. Res. 64B, 169–183.

Abers, G.A., Roecker, S.W., 1991. Deep structure of an arc–continent collision: earthquake relocation and inversion of upper mantle P and S wave velocities beneath Papua New Guinea. J. Geophys. Res. 96, 6379–6401.

Arculus, R.J., 2003. Use and abuse of the terms calcalkaline and calcalkalic. J. Petrol. 44, 929–935.

Berry, R.F., McDougall, I.A., 1986. $^{40}Ar/^{39}Ar$ and K/Ar dating evidence from the Aileu Formation, East Timor, Indonesia. Chem. Geol. 59, 43–58.

Chappell, J., 1974. Geology of coral terraces, Huon peninsula, New Guinea: a study of Quaternary tectonic movements and sea-level changes. Bull. Geol. Soc. Am. 81, 17–38.

Cooper, P., Taylor, B., 1987. Seismotectonics of New Guinea: a model for arc reversal following arc–continent collision. Tectonics 6, 53–67.

Crook, K.A., 1987. Petrology and mineral chemistry of sedimentary rocks from the western Solomon Sea. Geo Mar. Lett. 6, 203–209.

Denham, D., 1969. Distribution of earthquakes in the New Guinea–Solomon Islands region. J. Geophys. Res. 74, 4290.

Dow, D.B., 1977. A geological synthesis of Papua New Guinea. BMR Aust. Geol. Geophys. Bull. 201 (41 pp).

Eggins, S.M., Woodhead, J.D., Kinsley, L., Mortimer, G., Sylvester, P., McCulloch, M.T., Hergt, J.M., Handler, M., 1997. A simple method for the precise analysis of 40 or more trace elements in geological materials by ICPMS using enriched isotope internal standardisation. Chem. Geol. 134, 311–326.

Elburg, M.A., Foden, J.D., van Bergen, M.J., Zulkarnain, I., 2005. Australia and Indonesia in collision: geochemical sources of magmatism. J. Volcanol. Geotherm. Res. 140, 25–47.

Gill, J.B., 1981. Orogenic Andesites and Plate Tectonics. Springer, Berlin, p. 358.

Gill, J.B., Morris, J.D., Johnson, R.W., 1993. Timescale for producing the geochemical signature of island arc magmas: U–Th–Po and Be–B systematics in recent Papua New Guinea lavas. Geochim. Cosmochim. Acta 57, 4269–4283.

Hall, R., Spakman, W., 2002. Subducted slabs beneath the eastern Indonesia–Tonga region: insights from tomography. Earth Planet. Sci. Lett. 201, 321–336.

Hill, K.C., Gleadow, A., 1989. Uplift and thermal history of the Papuan Fold Belt, Papua New Guinea: apatite fission track analysis. Aust. J. Earth Sci. 36, 515–539.

Jakes, P., Gill, J.B., 1970. Rare earth elements and the island arc tholeiite series. Earth Planet. Sci. Lett. 9, 17–28.

Johnson, R.W., 1977. Distribution and major element chemistry of late Cenozoic volcanoes at the southern margin of the Bismarck Sea, Papua New guinea. Australian Bureau of Mineral Resources Report, vol. 188.

Johnson, R.W., 1979. Geotectonics and volcanism in Papua New Guinea. BMR J. Aust. Geol. Geophys. 4, 181–207.

Johnson, R.W., Chappell, B.W., 1979. Chemical analyses of rocks from the late Cenozoic volcanoes of north-central New Britain and the Witu Islands, Papua New Guinea. Australian Bureau of Mineral Resources Report, vol. 209.

Johnson, R.W., Jaques, A.L., 1980. Continent–arc collision and reversal of arc polarity: new interpretations from a critical area. Tectonophysics 68, 111–124.

Martinez, F., Taylor, B., 1996. Back-arc spreading, rifting, and microplate rotation between transform faults in the Manus Basin. Mar. Geophys. Res. 18, 203–224.

McCaffrey, R., 1989. Seismological constraints and speculations on Banda arc tectonics. Neth. J. Sea Res. 24, 141–152.

McDermott, F., Defant, M.J., Hawkesworth, C.J., Maury, R.C., Joron, J.L., 1993. Isotope and trace element evidence for three component mixing in the genesis of the North Luzon arc (Philippines). Contrib. Mineral. Petrol. 113, 9–23.

Northard, S., Haines, J., Jackson, J., Holt, B., 1996. Distributed deformation in the subducting lithosphere at Tonga. Geophys. J. Int. 127, 328–338.

Pegler, G., Das, S., Woodhouse, J.H., 1995. A seismological study of the eastern New Guinea and western Solomon Sea regions and its tectonic implications. Geophys. J. Int. 122, 961–981.

Plank, T., 2005. Constraints from thorium/lanthanum on sediment recycling at subduction zones and the evolution of the continents. J. Petrol. 46, 921–944.

Powell, R.P., Woodhead, J.D., Hergt, J.M., 1998. Uncertainties in Pb isotope analysis: deconvolution in the double spike method. Chem. Geol. 148, 95–104.

Richards, J.R., 1986. Lead isotopic signatures: further examination of comparisons between South Africa and Western Australia. Trans. Geol. Soc. S. Africa 89, 285–304.

Sandiford, M., 2008. Seismic moment release during slab rupture beneath the Banda Sea. Geophys. J. Int. 174, 659–671.

Tregoning, P., Lambeck, K., Stolz, A., Morgan, P., McClusky, S.C., van der Beek, P., McQueen, H., Jackson, R.J., Little, R.P., Laing, A., Murphy, B., 1998. Estimation of current plate motions in Papua New Guinea from Global Positioning System observations. J. Geophys. Res. 103, 12,181–12,203.

Tregoning, P., McQueen, H., LAmbeck, K., Jackson, R., Little, R., Saunders, S., Rosa, R., 2000. Present-day crustal motion in Papua New Guinea. Earth Planets Space 52, 727–730.

Van Bergen, M.J., Vroon, P.Z., Hoogewerff, J.A., 1993. Geochemical and tectonic relationships in the east Indonesian arc–continent collision region: implications for the subduction of the Australian passive margin. Tectonophysics 223, 97–116.

Wallace, L.M., Stevens, C., Silver, E., McCaffrey, R., Loratung, W., Hasiata, S., Stanaway, R., Curey, R., Rosa, R., Taugaloidi, J., 2004. GPS and seismological constraints on active tectonics and arc–continent collision in Papua New Guinea: implications for mechanics of microplate rotations in a plate boundary zone. J. Geophys. Res. 109, B05404.

Widiyantoro, S., Van der Hilst, R., 1997. Mantle structure beneath Indonesia inferred from high-resolution tomographic imaging. Geophys. J. Int. 130, 167–182.

Woodhead, J.D., Johnson, R.W., 1993. Isotopic and trace element profiles across the New Britain island arc, Papua New Guinea. Contrib. Mineral. Petrol. 113, 479–491.

Woodhead, J.D., Eggins, S.M., Gamble, J.G., 1993. High field strength and transition element systematics in coupled arc-back arc settings: evidence for multi-phase melt extraction and a depleted mantle wedge. Earth Planet. Sci. Lett. 114, 491–504.

Woodhead, J.D., Volker, F., McCulloch, M.T., 1995. Routine Pb isotope determinations using a ^{207}Pb–^{204}Pb double spike: a long-term assessment of analytical precision and accuracy. Analyst 120, 35–39.

Woodhead, J.D., Eggins, S.M., Johnson, R.W., 1998. Magma genesis in the New Britain island arc: further insights into melting and mass transfer processes. J. Petrol. 39, 1641–1668.

Woodhead, J.D., Hergt, J.M., Davidson, J.P., Eggins, S.M., 2001. Hafnium isotope evidence for 'conservative' element mobility during subduction zone processes. Earth Planet. Sci. Lett. 192, 331–346.

Yang, T.F., Lee, T., Kurz, M.D., 1994. Geochemical variations along the North Luzon arc (Taiwan): an example of arc magmatism during arc–continent collision. Geol. Soc. Am. Abstr. Progs. 26, 274.